EXPERIMENTAL STUDY ON ASEISMIC BEHAVIORS OF BRICK BUILDINGS

Xia, Jingqian (I)
Chen, Maogong (II)
Presenting Author: Xia, Jingqian

SUMMARY

In the paper tests of aseismic behaviors of brick masonry and full-scale masonry buildings under static and dynamic loading are described, results including the failure characteristics of masonry building, the influence of compressive stress on shear strength, the variation of dynamic behavior of masonry building before and after failure, the effect of strengthening and the basic dynamic characteristics of brick masonry are given.

INTRODUCTION

With advantages of local material, low cost etc, brick building is still the type of structures widely used in the present public buildings in China. It's shown in the survey of earthquake damages that the aseismic capacity of such buildings is very low. Thus the experimental study of the dynamic behavior of brick masonry as well as the masonry building and its improvement is very important. In this paper results of static and dynamic tests of full-scale masonry buildings and brick masonry are described. The tests were aimed at studying of failure characteristics of full-scale model, effect of normal stress on shear strength of the wall, changing of the dynamic behavior of building before and after failure, basic dynamic characteristics of the brick masonry, and the function of the horizontal strengthening. etc.

FULL-SCALE MODEL TEST OF BRICK BUILDINGS

The building models tested included 4 two-story single buildings of the same size (see Fig. 1). Walls were made of clay bricks with strength of 75 kg/cm^2 and cementlime mortar with strength of 25 kg/cm^2. Floors and roofs were precast slabs. Besides, there was a R.C. collar beam on each floor. Strip foundations of the buildings laid by rugged stone were connected each other. In model No. 4 the transversal walls were strengthened by 3 R.C. collar belts on the top floor and reinforced with steel bars on the ground floor as shown in Fig. 1.

Of the 4 models, No. 1, 2, and 4 were used to carry out the lateral loading test, and No. 3 for dynamic test.

Lateral Loading Test

In order to simulate the actual low-rise building various amount of iron blocks was placed on each floor so as to the expected normal stress being resulted in the walls (see Tab. 1.)

(I)(II) Research Associate, Institute of Engineering Mechanics, Academia Sinica, Harbin, China.

During test, a uniaxial horizontal load was applied to the collar beam by a hydraulic jack on each floor, using the adjacent model as the support of the jack. The top and ground floors were tested separately for all models.

The hydraulic jack produced cyclic load in one direction, maximum value of loading of the latter cycle was 2 T greater than that of the previous one. In sucha manner the laoding increased step by step up to failure occurring in the wall. After failure one or two cycles were applied to observe the slip resistance of the walls.

Test shows that transversal wall of the model, subjected to shear force, failed first, without obvious plastic deformation cracks along brick joints suddenly occurred in the diagonal direction of the wall, beginning in the central part and then extending to two opposite directions to the wall corners as shown in Fig. 2. With load increasing cracks extended horizontally to the longitudinal walls. Such damage pattern agrees with that observed in earthquakes. In model No.4 due to the existing of 3 R.C. belts in the wall of the upper floor the occurrence of inclined crack passing through the wall was prevented, only in the lowest part of the wall some slightly inclined cracks appeared. However, on the reinforced brick wall of the ground floor, several inclined cracks occurred (see Fig. 2b)

The measured strain distribution of the wall, as shown in Fig. 3, agrees well with the pattern of the cracks.

Tab. 1. indicates that the normal pressure increased from 0.59 kg/cm^2 to 2.15 kg/cm^2, the average shearing strength increased from 1.1 kg/cm^2 to 2.07 kg/cm^2, which demonstrates obvious increasing of shearing strength of the wall with compression. (see Fig. 4)

Test indicates that the relative-story displacement at the top floor of models No. 1 and 2 is 1.82mm in average at initial cracking and 2.0mm when ultimate loading just arrives, for model No. 4 they are 2.07mm and 4.87mm respectively.

The displacement at the top of the wall due to translation and rocking of the foundation is about 20 to 60 percent of the total displacement. Fig. 5a shows the P-Δ curves. Note that it is in general nonlinear except the initial segment and the plastic stage is not evident, for some walls it is even difficult to distinguish the initial cracking load and ultimate load. Fig. 5b shows P-Δ curves of model No. 1 & 4 without or with strengthening. The initial cracking load and ultimate load of the ground and top floor are increased for model No. 4, comparing with No. 1 Furthermore, Model No. 4 significantly differs from No. 1 in longer portion of slipping (4$\sim$8 mm) without considerable decreasing of load.

The horizontal load being applied only in one direction, the story stiffness of the model is defined as

$$K = \frac{\text{max. load}}{\text{corresponding max. displacement}}$$

Fig. 6 is the stiffness degradation curves, indicating that the stiffness when crack appears is decreased by 60% than the initial stiffness. However, decreasing of stiffness after cracking is not significant.

Definning the ductility factor C as the ratio of maximum story-displacement sustained by the ultimate load and the story-displacement when ultimate load just reaches, we obtain C equal to 1 for various floor of model No. 1 and 2 and equal to 1.65 for ground floor of model No. 4.

A comparison of model No.1 and 4 shows that the strengthening of the wall increases shear resistance by 28% and 10% respectively by using R.C. collar beams and reinforced steel bars under the same normal pressure, while the ultimate deformation increases 61.5% and 101% respectively for the above two types of strengthening, demonstrating the adopted strengthen methods has a markable effect on improvement of ductility.

Dynamic Testing

An eccentric mass-type generator located on the roof of the model building No.3 has been used to produce horizontal force. The exciting frequencies vary from 1 to 10 cps. When it was 6.3 cps there happened some slide between two precast slabs of the roof and horizontal crack on the ground surface at about 1 m from the foundation, which resulted in the decreasing of stiffness of the model and resonance occurred at 7.3 cps. The maximum horizontal force reached was 7.9^{T}.

Fig. 7 illustrates the measured and calculated lateral displacement distribution of the model building. Calculation was based on multi-degree-of freedom system on elastic foundation. Note that the building behaves as a cantilever shear beam fixed on the elastic foundation. The amplitude of the building model is small, the magnitudes of the displacement due to rocking and translation of the foundation have the same level and they together constitute 25 to 50% of the total displacement, similar to that obtained from the static loading test as indicated before.

The natural frequencies before and after failure of the building measured through micro-tremor and explosion are summarized in Tab. 2. From the Table it can be seen that the buildings tested are characterized by their high stiffness and short natural period. The fundamental period in N-S is a little lower than that in W-E due to the holl's weakening effect. The natural frequencies were decreased by 32~35% after penetration crack occuring in the wall and by 16~20% in the perpendicular N-S direction.

The damping ratio of the tested buildings varies in interval 0.023~0.10. Results obtained from model No. 3 show that the damping ratio increases after failure.

BASIC MECHANICAL PROPERTIES OF BRICK MASONRY UNDER AXIAL COMPRESSIVE LOADING

Specimens and Test Method

To study the static and dynamic behavior of the brick masonry 26 prismatic specimens with dimension 37×49×106 cm had been tested. Tests were performed on a 50 T fatigue testing mechine. In dynamic testing, 5 T of static load was applied to the specimen first, and then simple harmonic load of 4 cps frequency was supperposed. During test the load increased stage by stage till some maximum value and then decreased to form a cycle. The duration of the sustained load at every stage was 30 sec. After 3~5 cycles load increased until the specimen failed. The loading sequence both in static and dynamic test was the same for the sake of comparison.

Results and Analysis

The values of the basic parameters obtained from tests are given in Tab. 3. From the Table we see that the static and dynamic (under low frequency) compressive strength are nearly the same and close to the specified values in Code of China.

As the Code of China specifies the safety factor of masonry in compression to be 2.3, i.e. stress applied to the masonry must not exceed 0.43 times of its compressive strength in normal condition, therefore, it is reasonable to take the secant modulus at $\sigma/R = 0.43$ (here is the compresive stress, R the compressive strength) as Young's modulus of brick masonry. From Tab. 3 it is shown that dynamic Young's modulus is higher than the static modulus. Part result of tests for the same specimen is listed in Tab. 4, from which we have $E_d = 1.47\ E_s$ where E_d and E_s are dynamic and static modulus respectively.

The plots of Poisson ratio of brick masonry versus stress ratio σ/R are similar for dynamic and static condition as shown from Fig. 9. Before initial cracking the variation of Poisson ratio is not significant, but once crack occurs, it increases abruptly, while it is of no sense. The value of 0.15 corresponding to $\sigma/R = 0.43$ may be taken for both dynamic and static condition.

Fig. 10 is a plot of damping ratio of six specimens versus stress ratio obtained from the area of hystersis loop in tests. The damping ratio varies from 0.01 to 0.05. There is a trend of increase of damping ratio with stress amplitude.

CONCLUDING REMARKS

From the test results the following conclusions can be drawn;

a. Masonry building always cracks suddenly without obvious yielding. Its shear deformation is very small. During initial cracking the relative displacement induced by shear deformation is about 0.6 mm/m.

b. Even though the range of variation of compressive stress in the test is very small, shear strength obviously increases with compressive stress. The effect of compressive stress on ductility of brick masonry is not evident.

c. The basic feature of multiple-story masonry building is the high stiffness and short natural period. The natural frequence decreases by 32-35% after initial cracking. Damping ratio varies in interval 0.01 to 0.05 for brick masonry and 0.023 to 0.1 for masonry building due to the inclusion of soil and radiation damping of the foundation.

d. Under low-frequency loading the dynamic compressive strength of brick masonry is nearly the same as that in static loading condition and is in accordance with that specified in the Code of China. Poisson ratio in dynamic condition also very closes to that in static condition and takes the value of 0.15. Test shows Young's modulus under dynamic loading is about 1.5 times that under static loading.

e. Aseismic strengthening, such as horizontal R.C. belts is effective and applicable in practice, such measurements not only increase the ultimate bearing capacity of the masonry building, but more importantly improve its ductility.

Table 1

Model No.	Rm kg/cm²	σ	Pc T	Pu T	τ_c	τ_u	Δ_c N	Δ_c S	Δ_u N	Δ_u S	Pc/Pu
1u	32	0.59	11.20	11.20	1.10	1.10	1.30	2.97	1.30	2.97	1.00
2u	28.5	0.98	13.45	13.45	1.32	1.32	1.13	1.06	1.53	1.38	1.00
1d	37.5	1.36	18.72	19.60	1.81	1.93	1.45	2.47	1.48	2.56	0.94
2d	31.	2.15	20.65	21.00	2.03	2.07	2.15	1.99	2.17	2.43	0.98
4u	35.5	0.59	13.75	14.40	1.36	1.41	2.36	2.57	2.55	3.78	0.96
4d	35.5	1.36	19.50	21.60	1.91	2.12	2.12	1.19	4.56	3.17	0.90

Note: 1. Values in the table are the average value of the North and South wall.

2. Rm — Mortar strength; σ — compressive stress in kg/cm²;
Pc — load at initial cracking;
Pu — ultimate load; τ — shear stress in kg/cm²;
Δ_c — displacement at initial cracking in mm.
Δ_u — displacement when ultimate loading just arrives in mm.

Table 2

			No. 1 W-E	No. 1 S-N	No. 2 W-E	No. 2 S-N	No. 3 W-E	No. 3 S-N	No. 4 W-E	No. 4 S-N
Frequency	bef. fuil	micr-tre	10	8.9	8.5	7.4	10	8.9	9.8	7.5
		expl.			8.6	8.1	9.8	8.7	10	7.5
	aft. fuil	micr-tre	6.44	7.05	6.5	6.0	7.3		6.6	6.3
Damping ratio	bef. fuil					0.036	0.023 ~ 0.096	0.041		0.0814
	aft. fuil		0.084	0.0525			0.123			

Tab. 3

Type Loading	Model No.	Rm	Rp	$\overline{Rp}$	Pc / T	Pu / T	ε_c	ε_u	E	$\overline{E}$	μ	$\overline{\mu}$
Static	1	25	24.82		30.2	45.0	955	1572	1.85		0.145	
	2	25	22.06	22.43	35.0	40.0	712	1686	2.90	2.48	0.130	0.145
	3	25	20.40		30.0	37.0	594	881	2.70		0.160	
	10	50			>50.0						0.190	
	11	50	27.89	27.93	45.0	50.6	1151	1794	4.85	4.70	0.140	0.143
	12	50	27.96		45.0	50.7	663	1010	4.55		0.100	
Dynamic	4	25	20.96		33.0	38.0			2.45		0.180	
	5	25	14.62		23.5	26.5	531	671	2.49		0.170	
	6	25	17.76			32.2						
	7	25	23.17		35.0	42.0	581	1171	4.76	3.92	0.160	0.153
	8	25	23.44		28.0	42.5	374	1031	4.94		0.148	
	9	25	19.31	21.29	32.0	40.0	453		4.16		0.084	
	19	25	25.46		38.5	46.6	605	1373	3.69		0.170	
	20	25	24.26		30.0	44.0	498	2020	4.96		0.160	
	23	25	19.70		26.5	35.7	493	683	3.22			
	24	25	24.60		31.0	44.6	518		3.45	3.76		
	25	25	19.30		26.5	34.5	444		3.64			
	26	25	22.89		26.5	41.5	345		3.97			
	13	50	27.50		41.0	50.0	639	956	4.43		0.127	
	14	50	28.10		46.0	51.0	541	603	5.01		0.097	
	15	50	28.10		38.0	51.5	439	860	6.87		0.146	
	16	50		28.05	>50.0					5.66	0.148	0.142
	17	50			>50.0		528		5.95		0.130	
	18	50	28.40		40.0	51.5	603	1164	5.28		0.100	
	21	50	28.10		42.0	51.0	451		6.67			
	22	50	28.10		35.0	51.0	531		5.40		0.243	

Tab. 4

Comp. stress	Model	E_d	E_s	E_d/E_s
2.76	23	2.63	2.05	1.28
	24	4.32	2.83	1.52
	25	3.02	2.77	1.09
	26	3.34	3.03	1.00
5.52	23	2.90	2.71	1.34
	24	4.32	2.35	1.58
	25	3.66	2.27	1.60
	26	4.13	2.44	1.69
8.27	23	3.22	2.30	1.39
	24	3.45	1.90	1.81
	25	3.64	1.82	2.00
	26	3.97	2.60	1.53
Average		3.50	2.38	1.47

Natation:

R_m -Mortar strength in kg/cm^2

R_p - Compressive strength in kg/cm^2

ε_c - Strain at initial cracking in 10^{-6}

ε_u - Strain at ultimate loading in 10^{-6}

E - Modulus in 10^4 kg/cm^2

μ - Poisson ratio

$\overline{(\ )}$ - The average of ( )

Other natations see Tab. 1

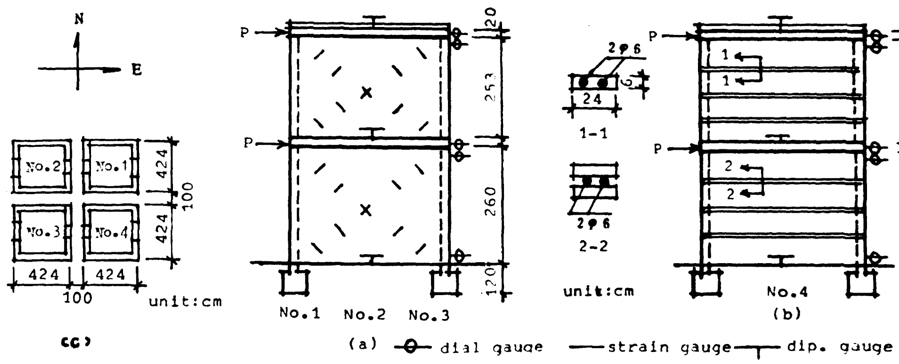

Fig. 1

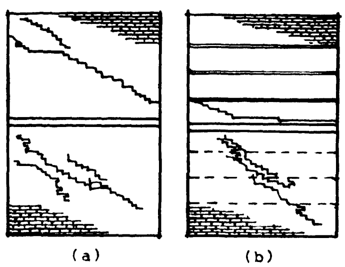

Fig.2

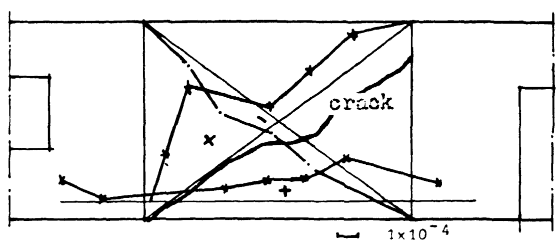

Fig.3

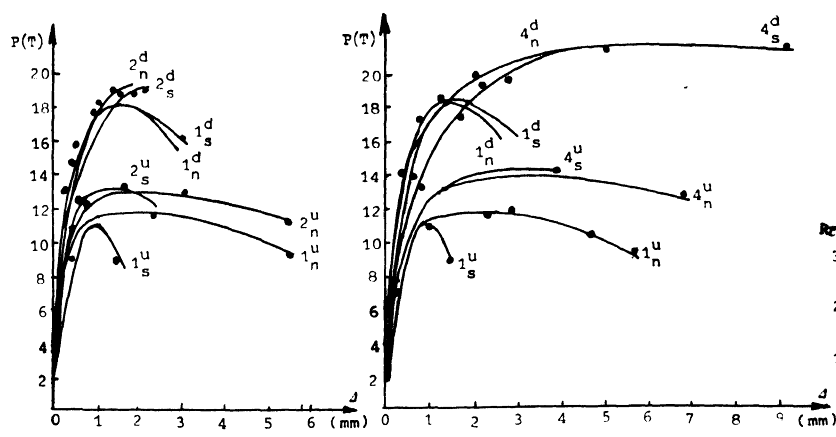

Fig.5

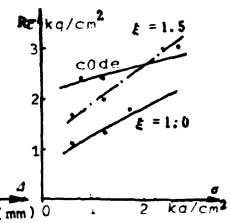

Fig.4

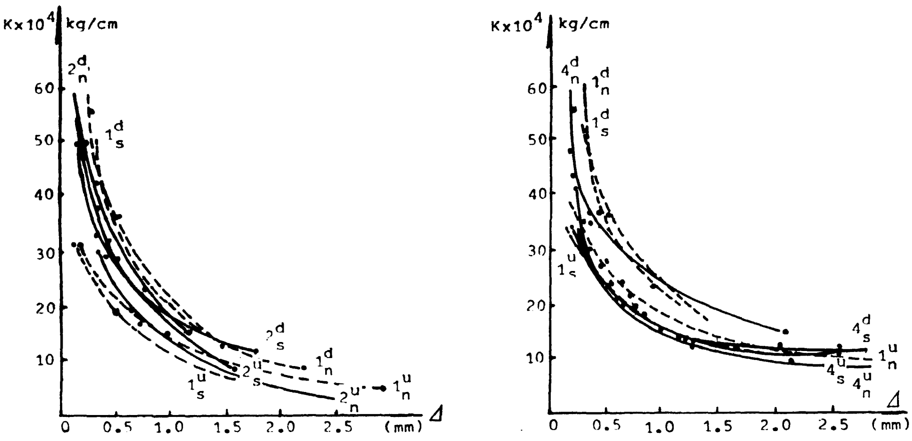

(a) (b)

Fig.6

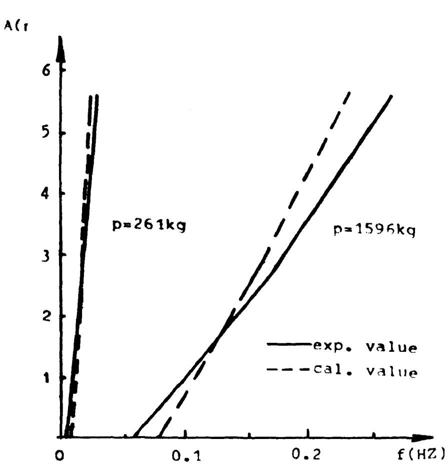

Fig.7

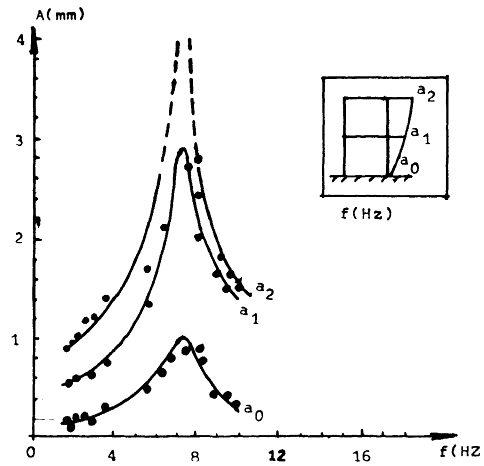

Fig.8

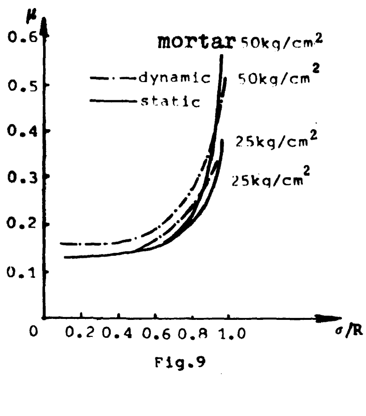

Fig.9

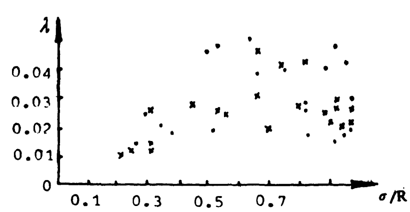

Fig.10